JOURNAL OF SOLID STATE CHEMISTRY 29, 345–354 (1979)

A Thermodynamic Study of Sodium-Intercalated TaS_2 and TiS_2

ALAN S. NAGELBERG* AND WAYNE L. WORRELL

Department of Metallurgy and Materials Science K1, University of Pennsylvania, Philadelphia, Pennsylvania 19104

Received November 3, 1978

The variation of the sodium chemical potential (μ_{Na}) with composition x in Na_xTaS_2 and Na_xTiS_2 has been measured electrochemically using propylene carbonate-based and β-alumina electrolytes. At 300°K the sodium chemical potential in Na_xTaS_2 varies from −63 to −25 kcal/mole as x increases from 0.003 to 0.92, respectively. Within experimental uncertainty, the compositional variation of μ_{Na} was linear. In Na_xTiS_2, the sodium chemical potential varies from −60 to −36 kcal/mole as x increases from 0.001 to 1.0, respectively. The compositional variation of μ_{Na} in Na_xTiS_2 exhibits two plateaus indicative of two-phase regions for $0.2 \leqslant x \leqslant 0.35$ and $0.6 \leqslant x \leqslant 0.7$. The standard free energies of intercalation for sodium-intercalated TaS_2 and TiS_2 are less negative than those reported for the respective lithium-intercalated compounds. The standard free energy of intercalation becomes more negative for both the sodium- and lithium-intercalated compounds as the dichalcogenide changes from TaS_2 to TiS_2.

Introduction

The dichalcogenides of the Group IV, V, and VI transition metals have received considerable attention in recent years because of their unique properties (*1–12*). The dichalcogenides form compounds with layered structures in which a hexagonal array of transition metal atoms (M) are sandwiched between two hexagonal layers of chalcogen atoms (X) as shown in Fig. 1a. The transition metal atoms have either a trigonal prismatic (Fig. 1b) or octahedral coordination (Fig. 1c) of chalcogen atoms. The X–M–X layers are used as building blocks to form the crystalline lattice. The interesting feature of this structure is the weak bonding between chalcogen atoms of adjacent X–M–X layers that allows the easy insertion or intercalation of atoms or molecules between the layers. Only elements or molecules that readily donate electrons have been intercalated at present. The donation of electrons to the MX_2 layers by intercalated species has been confirmed for the alkali metal intercalates by NMR studies (*9, 10*). For more details of the structures and chemical properties of the intercalated dichalcogenides, the reader is referred to an excellent review by Whittingham (*11*).

Of particular interest to this study are sodium-intercalated tantalum disulfide and titanium disulfide. Omloo and Jellinek (*12*) formed Na_xTaS_2 by reacting TaS_2 powder with sodium at 800°K in evacuated quartz capsules. A single-phase solid solution was reported to exist between $x = 0.4$ and $x = 0.67$. The upper limit was determined by an undesirable reaction between sodium and the quartz capsules. The c-axis spacing per layer of the hexagonal TaS_2 crystals was observed to change from 6.04 to 7.29 Å during intercalation. Matsumoto *et al.* (*13*) intercalated sodium into TaS_2 using a sodium

* Presently at Sandia Laboratories, Livermore, Calif. 94550.

0022-4596/79/090345-10$02.00/0

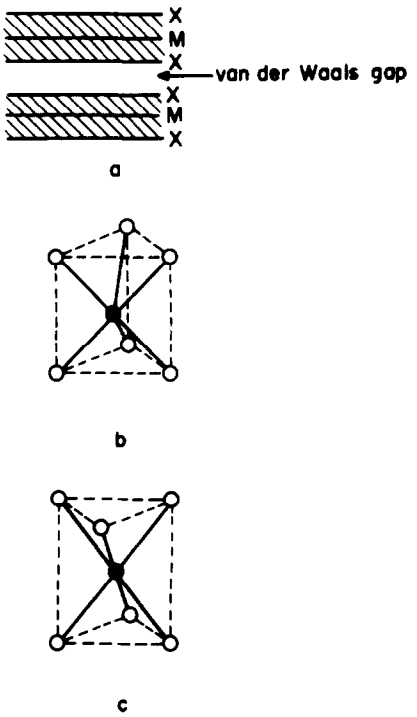

FIG. 1. (a) Stacking sequence of M and X planes. (b) Trigonal prismatic coordination. (c) Octahedral or trigonal antiprismatic coordination.

hexamethyl phosphoric triamide (HMPA) solution and measured the X-ray lattice parameters. Their measurements, $a = 3.34$ Å and $c = 14.37$ Å, for the 2H form, are in good agreement with Omloo and Jellinek.

Rouxel *et al.* (*7*) intercalated sodium into TiS_2 using solutions of sodium dissolved in liquid ammonia. Three distinct phases were reported. A subsequent NMR study by Silbernagel and Whittingham (*10*) indicated multiphase behavior of Na_xTiS_2, but the composition ranges for the phases do not correspond exactly with those observed by Rouxel *et al.* The observed Knight shifts are 20–80 ppm compared to 1120 ppm for pure sodium, indicating a very small electron character at the sodium nucleus.

The thermodynamics of only one sodium-intercalated disulfide has been studied previously. Winn *et al.* (*14*) found that the chemical potential of sodium in Na_xTiS_2 was a nonlinear function of composition with constant voltage regions at compositions around $x = 0.35$ and $x = 0.75$. For compositions greater than $x = 0.45$, the measured sodium chemical potential was a function of the titanium disulfide nonstoichiometry.

The ease of, and short times required for, intercalation indicates that the inserted species has a high mobility (*11*). Therefore the dichalcogenides which exhibit high electronic conductivities (*15, 16*) show promise as electrode materials in room temperature cells. In this study the compositional variation of the sodium chemical potential in Na_xTaS_2 and Na_xTiS_2 has been measured to assess their electrode capabilities and to analyze the nature of chemical bonding in these compounds.

Experimental

In order to avoid contamination by oxygen or moisture, intercalation of disulfide powders and their subsequent handling were performed in a Vacuum Atmospheres glove box with either an argon or an argon–5% hydrogen atmosphere. The water content of the atmosphere within the glove box was typically 1 ppm H_2O.

Tantalum disulfide, obtained from Cerac/Pure, Inc., typically had the composition $Ta_{1.1}S_2$ and was further annealed with sulfur to obtain the stoichiometric 2H polytype (*11, 17*). Sulfur was added by two methods. In the first, nonstoichiometric TaS_2 was annealed at 850°K in a prepurified flowing argon stream (*18*) in which elemental sulfur was placed upstream at 425–525°K. After annealing, the TaS_2 powder was cooled in the furnace. In the second method, nonstochiometric TaS_2 was sealed in an evacuated quartz capsule with excess sulfur. The capsule consisted of two separate compartments for S and TaS_2 with a small neck between compartments. The quartz capsule was then heated in a temperature gradient so the TaS_2 powder was at 850°K,

and the sulfur part of the capsule was at ~600°K. Such a procedure allowed the powder to be equilibrated with a high-equilibrium sulfur pressure while any excess sulfur was condensed out at the cool end.

The stoichiometry of the TaS_2 powders after annealing was checked by combustion of the sulfide powders to Ta_2O_5 in a tared porcelain crucible. Powders were slowly heated in air to 1073°K to avoid flaming and loss of powder. The stoichiometry of the annealed powder, obtained from the weight change and final weight for TaS_2, was $Ta_{1.01\pm0.005}S_2$. The stoichiometry of TiS_2 powders obtained from Cerac/Pure, Inc., was found to be $Ti_{1.006}S_2$ by an analogous analysis, and further annealing of TiS_2 was unnecessary.

Sodium can be intercalated into the disulfides using a variety of methods (*1, 11, 19–23*). In this study, intercalation was accomplished by two methods, either electrochemically in the experimental cell or chemically using an organometallic solution. Sodium naphthalide dissolved in tetrahydrofuran (THF) was used as the organometallic intercalation agent (*23, 24*). Disulfide powders were immersed in solutions with varying sodium contents for 2–3 days. After this intercalation period, the intercalated powders were filtered out of the solutions, washed with THF, and dried. The sodium content of intercalated disulfides was determined from the sodium content of the sodium naphthalide solutions before and after intercalation (*25*). In this method 2-ml samples of the sodium naphthalide solutions are diluted with water to make a 1:1 solution. The diluted solution was titrated with standardized HCl to the endpoint of a phenolphthalein indicator to obtain the sodium content.

Cathode pellets were made by uniaxially compacting the sodium-intercalated powders at 30 000 psi in a 1-cm die for room temperature studies and a 0.64-cm die for elevated temperature measurements. Tantalum and titanium disulfides were compacted in a 1-cm-diameter die to form cylindrical pellets for X-ray diffraction studies with a Phillips–Norelco diffractometer with CuKα radiation. The compaction resulted in significant preferred orientation, and two angle scans were performed. One scan at low sensitivity was used to identify the position of the strong (00*l*) peaks. A second scan at slow speed (1/4°/min) and high sensitivity was used to identify other disulfide peaks and possible second-phase peaks. The observed diffraction patterns were compared with those reported in the literature (*26, 27*) to confirm the occurrence of only the 2H polytype in the annealed TaS_2 powders. For moisture- and oxygen-sensitive samples, a 0.5-mm glass capillary obtained from the Charles Supper Company, Cambridge, Massachusetts, was used in Debye–Scherrer cameras.

A propylene carbonate-based electrolyte was used for measurements at 300°K, and a β- or β''-alumina electrolyte was used for measurements at 435 and 495°K. Propylene carbonate (PC) obtained from Aldrich Chemical Corporation, contained ~100 ppm H_2O (*28*). The residual water was removed by mixing ~100 ml PC with freshly cut lithium metal chips in a 150-ml flask fitted with a ground joint. The PC and lithium chips were shaken for at least 4 days. The resulting black reaction product was filtered out in the glove box before storing the clear liquid. After this treatment, no moisture was detected by gas chromatography; the sensitivity of the gas chromatograph was 2–3 ppm H_2O (*28*). Sodium electrolyte salts (NaI or $NaPF_6$) were dried under vacuum (<10 μm) at 453°K for 4–5 days. The propylene carbonate-based electrolyte was made by adding enough dried salt to form a saturated mixture in each cell (~1.1 *M* for NaI and 0.86 *M* for $NaPF_6$). The β- and β'' (Li_2O-stabilized)-alumina electrolytes were used for elevated temperature measurements. The β-alumina electro-

lytes were obtained from TRW as disks (~5 mm thick and ~2.5 cm in diameter). A method developed at the University of Utah (*29*) was used to prepare Li_2O-stabilized β''-alumina electrolytes. The electrolyte disks were machined to a 1-cm diameter and polished through 1 μm diamond paste to obtain a flat surface.

Two cell designs were used for electrochemical measurements using propylene carbonate-based electrolytes. The first cell shown in Fig. 2 was used with the intercalated tantalum disulfide cathodes. A cathode pellet (A) uniaxially compacted at 30 ksi was spring loaded between two 304 stainless-steel disks (B). Compacted cathodes had densities greater than 85% of the theoretical density. A stainless-steel rod (C) threaded into the upper disk was used to suspend the cathode in the liquid electrolyte and served as the electrical lead to the cathode. Two sodium anodes were used (D), one as a counter electrode and one as a reference electrode for subsequent diffusion studies. The anodes and cathode were electrically isolated by a Teflon spacer (E). All electrical leads went through another Teflon spacer (F) sealed with epoxy to the female member of a 34/45 ground glass joint (G). The seal was checked for vacuum tightness with a helium leak detector. The electrolyte was contained in a 34/35 ground joint sealed at one end (H). Cells were assembled in the glove box using a Teflon sleeve on the ground joint and removed from the glove box for measurements. When removed from the glove box, the ground glass joint was further sealed with G.E. RTV silicone rubber. Cells removed from the glove box were held in a constant temperature bath controllable to ±0.5°K. The temperature (±0.05°K) was measured using a mercury thermometer.

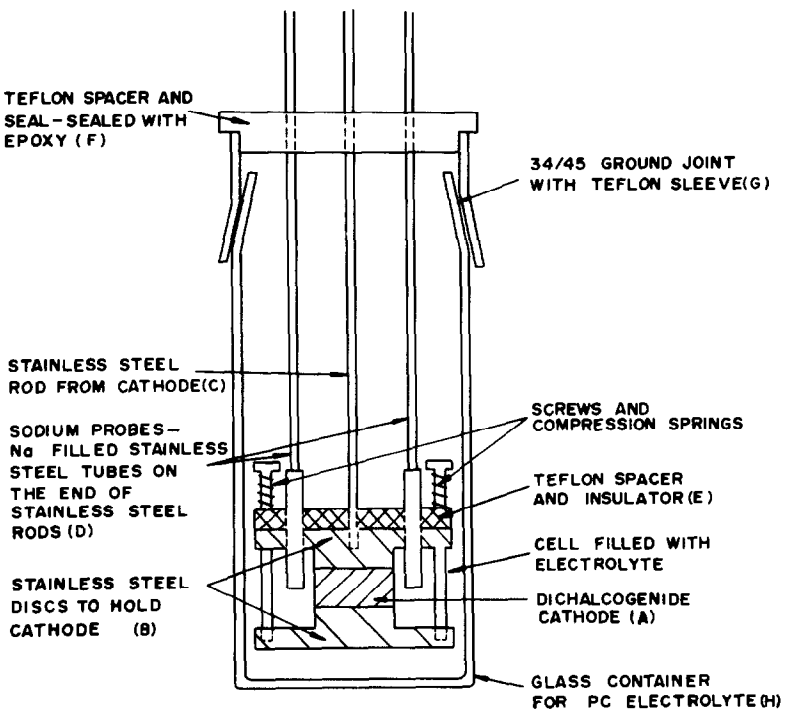

DESIGN OF PROPYLENE CARBONATE CELL

FIG. 2. Cell design for Na_xTaS_2 electrode.

Occasionally, compacted pellets of Na_xTaS_2 would disintegrate upon immersion into the propyelene carbonate-based electrolyte. When the recovered powders were rewashed with THF or PC and recompacted, the pellets of Na_xTaS_2 remained compacted when immersed in the electrolyte. Debye–Scherrer patterns of these powders showed no evidence of PC cointercalation.

Powders of Na_xTiS_2 did not remain compacted upon immersion in the electrolyte even after further washing and recompaction. Thus a second cell (Fig. 3) was designed to constrict the Na_xTiS_2 powders using a stainless-steel holder (B). The cathode (A) was intercalated powder compacted at 30 ksi into a 1-cm-diameter cylindrical recess in the stainless-steel holder (B). The holder has a $\frac{1}{8}$-in. stainless-steel rod (C) threaded into it which acts as an electrical lead. Glass fiber filter paper (D) separated the cathode from the solid sodium anode (E), compacted into a 1-cm-diameter hole in a stainless-steel disk (F). A stainless-steel plate (G) was used on the bottom of the anode. The sodium anode was held against the separator by two screws, one of which extended to form the electrical lead to the anode (H). A Teflon spacer (I) was used to maintain electrical isolation. This cell design was used in the glove box, and a 25-ml beaker was used as the electrolyte container.

In elevated temperature measurements using $\beta(\beta'')$-alumina electrolytes, the liquid sodium anode was contained in a flanged stainless-steel tube with the polished $\beta(\beta'')$-alumina electrolyte as the base. An annealed Pt gasket was used between the stainless-steel flange and electrolyte. The compacted powder cathode was $\frac{1}{4}$ in. in diameter and spring loaded to the bottom of the electrolyte disk. Platinum leads provided electrical contact to the cathode and anode.

The open-circuit voltages of the following two cells

$$\mathrm{Na(s)/Na^+\ (propylene\ carbonate)/Na_xTaS_2}$$
$$\text{or } Na_xTiS_2, \quad \text{(A)}$$

$$\mathrm{Na(l)/Na^+(\beta(\beta'')\text{-alumina})/Na_xTaS_2}, \quad \text{(B)}$$

were measured by using a high-impedance ($>10^9\ \Omega$) voltmeter or electrometer. After assembly, the open-circuit voltage was monitored until the voltage remained stable (± 2 mV) for 2 to 3 days. Occasionally the sodium content of the cathodes was changed by coulombic titrations at 50–300 $\mu A/cm^2$. The electrochemical titrations serve two purposes. First, they act as a check of the compositions determined analytically since the change of sodium content of the intercalated TiS_2 can be known precisely. Secondly, regions in which a constant open-circuit voltage is observed can be more carefully examined, especially for Na_xTiS_2. At the end of the coulombic titration, the cell voltage was again monitored until stable (± 2 mV) for 3 days.

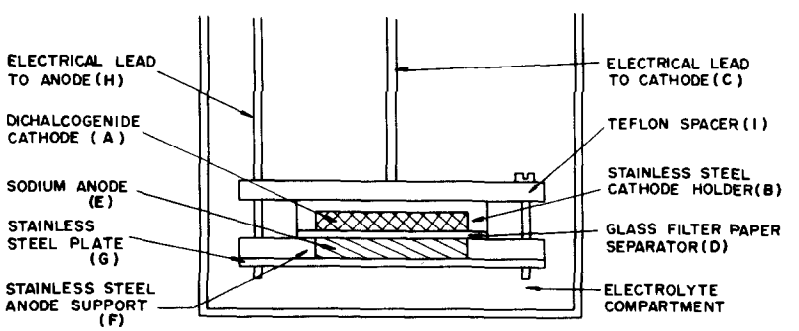

FIG. 3. Cell design for Na_xTiS_2 electrode.

Results and Discussion

The measured voltages for cell (A) with Na_xTaS_2 electrodes of variable composition are shown in Fig. 4. The open-circuit voltage, which decreases from 2.74 V ($x = 0.003$) to 1.08 V ($x = 0.92$), can be interpreted within the experimental uncertainty to exhibit either a linear variation with composition, x in Na_xTaS_2, or a voltage plateau when x is between 0.3 and 0.42, indicating a two-phase region. Although two-phase regions have been observed in the Na_xTiS_2 system (*7*), no crystallographic investigation of the Na_xTaS_2 system has been reported. Although future structural studies may indicate two-phase regions in Na_xTaS_2, a straight line does fit the data shown in Fig. 4 within an uncertainty (two standard deviations) of ±0.12 V. The straight line shown in Fig. 4 represents Eq. (1) which is obtained by a least-squares analysis.

$$E(\pm 0.12\ \text{V}) = 2.73 - 1.74\ \text{V}. \qquad (1)$$

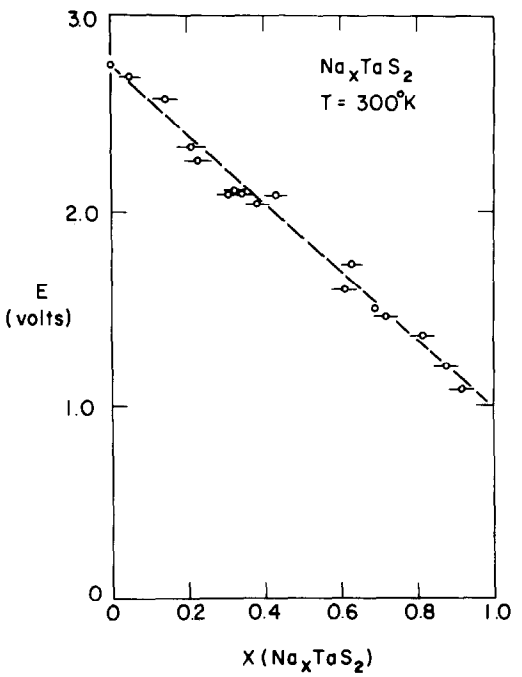

FIG. 4. Compositional variation of voltage of cell (A) with x in the Na_xTaS_2 electrode.

In Fig. 5, results from the solid-electrolyte cells [cell (B)] at 433 and 494°K are compared with Eq. (1). The cell voltages measured at these higher temperatures are within 0.04 V of those obtained from cell (A) at 300°K.

The open-circuit voltages measured for cell (A) using Na_xTiS_2 electrodes are shown in Fig. 6. Two voltage plateaus, indicative of two-phase regions, are observed in the composition ranges $0.2 \leqslant x \leqslant 0.35$ and $0.6 \leqslant x \leqslant 0.7$. At other compositions the voltage appears to vary linearly with x. Voltage plateaus could also be inferred to exist from similar electrochemical data obtained by Winn *et al.* (*14*) at 300°K. However, their open-circuit voltages are 0.2 to 0.3 V lower than those shown in Fig. 6. An $Na_{0.32}V_2O_5$ anode was used in Winn's cell, and the 0.2- to 0.3-V discrepancy could be due to uncertainties in the sodium chemical potential in $Na_{0.32}V_2O_5$.

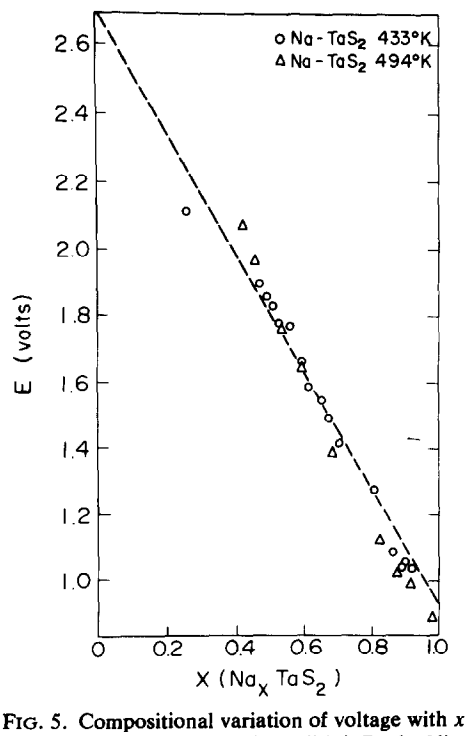

FIG. 5. Compositional variation of voltage with x in Na_xTaS_2 at 433 and 494°K using cell (B). Dashed line is Eq. (1) determined at 300°K using cell (A).

A crystallographic study of Na_xTiS_2 (*7, 30*) indicates that two-phase regions and constant voltage plateaus should be observed when x is <0.17, when x is between 0.33 and 0.38, and when x is between 0.67 and 0.79. Only a few results are shown in Fig. 6 when x is <0.2. Thus there are insufficient data to confirm the existence of a two-phase region, and a broken line is shown in Fig. 6 for when x is <0.17. The two voltage plateaus shown in Fig. 6 when x is between 0.2 and 0.35 and between 0.6 and 0.7 are not in agreement with the two-phase regions reported by Rouxel for Na_xTiS_2 (*7*). He reports that the phase transition at $x = 0.33$ ($x \simeq 0.2$ in this study) is a transition from a Stage II compound, with sodium intercalated in every other interlayer gap, to a Stage I compound, with sodium in every interlayer gap. The coordination of sodium in the Stage II compound was not determined, and it is not known whether the sodium coordination changes during the transformation to the Stage I compound, which exhibits a trigonal prismatic sodium coordination. The second reported phase transition for $x = 0.67$ (*30*) ($x = 0.6$ in this study) involves a change from trigonal prismatic to trigonal antiprismatic coordination of sodium atoms.

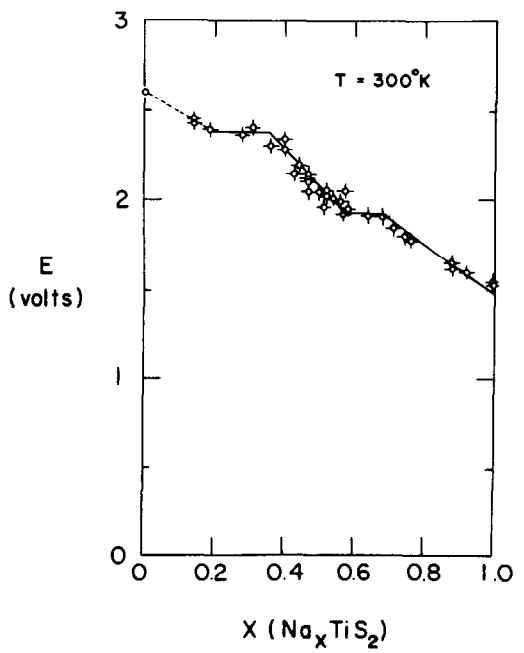

FIG. 6. Compositional variation of voltage with x in the Na_xTiS_2 electrode.

The disagreement in the phase boundaries in the Na_xTiS_2 system could be due to several reasons. A phase transition at room temperature should be very slow, particularly if it involves rearrangement of the titanium and sulfur atoms. Rouxel (*7*) used ammonia solutions to intercalate sodium into TiS_2. The effect of cointercalated ammonia in the interlayer gap or the effect of the subsequent heat treatment required to remove the ammonia has not been determined. Further studies are required to establish the exact compositional ranges for phases in the Na_xTiS_2 system.

Lithium-intercalated TiS_2 (*28*) and TaS_2 (*31*) cells exhibit larger open-circuit voltages and smaller compositional variations with x than their respective sodium-intercalated compounds. Among these four intercalated disulfides, only Na_xTiS_2 cells show a distinctly nonlinear compositional variation of voltage with x. A linear compositional variation of cell voltage indicates a single phase existing throughout the composition range in the intercalated disulfides. In this case, intercalated alkali metal atoms enter all the van der Waals gaps between S–*M*–S layers without changing the layer stacking sequence.

The standard free energy of intercalation, ΔG°_I, is a convenient parameter to compare the energy storage capabilities of the alkali metal-intercalated dichalcogenides as battery cathodes. The larger the standard free energy of intercalation, the larger will be the energy storage capacity of the electrode per mole. The standard free energy of intercalation, ΔG°_I, is defined as the free energy change accompanying the insertion of an alkali metal, A, into the Van der Waals gap of a transition metal dichalcogenide,

MX_2, as expressed by

$$xA + MX_2 \rightarrow A_xMX_2. \quad (2)$$

For reaction (2), one can write

$$\Delta G^\circ_I = -RT \ln K$$
$$= RT \ln a_{MX_2} + xRT \ln a_A \quad (3)$$

because $a_{A_xMX_2}$ is 1. One can express ΔG°_I for reaction (2) as

$$\Delta G^\circ_I = \Delta G^\circ_{A_xMX_2} - \Delta G^\circ_{MX_2} - x\Delta G^\circ_A. \quad (4)$$

Rewriting Eq. (4), the standard free energy of formation of A_xMX_2 is given by

$$\Delta G^\circ_{A_xMX_2} = \Delta G^\circ_I + \Delta G^\circ_{MX_2} \quad (5)$$

since ΔG°_A is zero. For the alkali metal-intercalated disulfides, the Gibbs–Duhem equation can be expressed as

$$0 = n_A\, d\mu_A + n_{MX_2}\, d\mu_{MX_2} \quad (6)$$

if the metal (M) to sulfur (S) ratio is constant. Rewriting Eq. (6) in the familiar integral form gives

$$\mu_{MX_2} - \mu^\circ_{MX_2} = RT \ln a_{MX_2}$$
$$= -\int_{\mu_A, n_A = 0}^{\mu_A, n_A = x} \frac{n_A}{n_{MX_2}}\, d\mu_A, \quad (7)$$

where by definition

$$\frac{n_A}{n_{MX_2}} = x \quad (8)$$

and

$$\mu_A - \mu^\circ_A = RT \ln a_{Na} = -FE \quad (9)$$

because $n = 1$ for an alkali metal.

Substituting Eqs. (8) and (9) into Eq. (7),

$$RT \ln a_{MX_2} = F \int_0^x x\, dE. \quad (10)$$

Substituting Eqs. (9) and (10) in Eq. (3),

$$\Delta G^\circ_I = -F\left[xE - \int_0^x x\, dE\right]. \quad (11)$$

Using the standard formula for integration by parts, Eq. (11) reduces to

$$\Delta G^\circ_I = -F \int_0^x E\, dx. \quad (12)$$

Thus, the standard free energy of intercalation is simply Faraday's constant times the area under the voltage composition curve from the pure disulfide to the intercalated compound. The standard free energy of formation of the compound A_xMX_2 from the elements is obtained by adding $\Delta G^\circ_{MX_2}$ to ΔG°_I [Eq. (5)].

The linear relationship given by Eq. (1) has been used to calculate values of the sodium chemical potential [Eq. (9)] and ΔG°_I [Eq. (12)] for Na_xTaS_2 at 300°K. These values are listed in Table I as a function of composition, x. The standard free energy of formation of TaS_2 at 300°K, obtained by extrapolation of high-temperature data (*32*) and using a standard state of solid sulfur, is -69 ± 3 kcal/mole. The standard free energy of intercalation of $Na_{1.0}TaS_2$ is -42.9 ± 1 kcal/mole (Table I), which gives a value of -111.9 ± 3.1 kcal/mole for the free energy of formation from the elements. Cell voltages shown in Fig. 6 have been used in Eq. (12) to obtain the values of sodium chemical potential and ΔG°_I for Na_xTiS_2 given in Table I. A value of $\Delta G^\circ_{TiS_2}$ of -94.6 ± 5 kcal/mole is obtained from the enthalpy (*33*) and entropy (*34*) at 300°K. The standard free energy of intercalation for $Na_{1.0}TiS_2$ is -48.4 ± 1 kcal/mole, which yields a value of -143.0 ± 5 kcal/mole for ΔG°_f of $Na_{1.0}TiS_2$ at 300°K.

A comparison of ΔG°_I for some lithium- and sodium-intercalated disulfides are given in Table II. The voltage measurements of Winn *et al.* were not considered since the measured sodium chemical potential of $Na_{0.32}V_2O_5$ is in question. The cell voltages for $LiTiS_2$ measured by Basu and Worrell (*28*) have been preferred over the values reported by Whittingham (*8*) since these

TABLE I

SODIUM CHEMICAL POTENTIAL AND STANDARD FREE ENERGY OF INTERCALATION FOR Na_xTaS_2 AND Na_xTiS_2 AT 300°K

	Na_xTaS_2		Na_xTiS_2	
Concentration (x)	μ_{Na} (kcal/mole)	$\Delta G°_I$ (kcal/mole)	μ_{Na} (kcal/mole)	$\Delta G°_I$ (kcal/mole)
0.1	−58.9	−6.1	−57.9	−5.9
0.2	−54.9	−11.8	−54.9	−11.6
0.3	−50.7	−17.0	−54.2	−17.0
0.4	−46.9	−22.0	−54.2	−22.4
0.5	−42.9	−26.5	−47.2	−27.4
0.6	−38.9	−30.5	−47.2	−32.0
0.7	−34.9	−34.2	−43.6	−36.5
0.8	−30.9	−37.5	−40.9	−40.7
0.9	−26.8	−40.4	−38.3	−44.7
1.0	−22.8	−42.9	−35.5	−48.4

authors do not know of any impurity or experimental phenomena that would cause higher cell voltages to be obtained. The intercalated titanium disulfide compounds have more negative standard free energies of intercalation than the intercalated tantalum disulfides. The lithium-intercalated compounds have more negative standard free energies of intercalation than sodium-intercalated compounds. A higher value of $\Delta G°_I$ corresponds to a higher average value of alkali metal chemical potential.

The observed linear variation of alkali metal chemical potential in the intercalated dichalcogenides over extended composition ranges is rather unusual. A thermodynamic model to be presented in a subsequent paper (*36*) relates the observed linear variation to the random occupation of vacant sites in the interlayer gap and to additional energy terms. It is found that the dominant energy terms are due to the repulsive interaction between inserted atoms and the compositional variation of the Fermi energy.

TABLE II

FREE ENERGIES OF INTERCALATION FOR VARIOUS LITHIUM- AND SODIUM-INTERCALATED DISULFIDES

Compound (reference)	$\Delta G°_I$ (kcal/mole)
$Li_{1.0}TiS_2$ (*28*)	−57.4
$Na_{1.0}TiS_2$[a]	−48.4
$Na_{1.0}ZrS_2$ (*24*)	−41.3
$Li_{1.0}VS_2$ (*35*)	−53.1
$Na_{1.0}$"NbS_2" (*24*)	−42.6
$Li_{1.0}TaS_2$ (*31*)	−50.5
$Na_{1.0}TaS_2$[a]	−42.9

[a] This study.

Acknowledgment

This material is based upon work supported by the National Science Foundation, MRL Program, under Grant No. DMR76-80994.

References

1. W. RUDORFF, *Chimia* **19**, 489 (1965).
2. "Physics and Chemistry of Materials with Layered Structures," Vols. 1–6, Reidel, Dordrecht (1976, 1977).
3. B. C. H. STEELE, *in* "Critical Materials Problems in Energy Production," Academic Press, New York (1976).
4. J. A. WILSON AND A. D. YOFFE, *Advan. Phys.* **18**, 193 (1969).

5. M. S. WHITTINGHAM, *in* "Electrode Materials and Processes for Energy Conversion and Storage" (J. D. E. McIntyre, S. Srinivasan, and F. G. Will, Eds.), The Electrochemical Society, Princeton, N.J. (1977).
6. F. R. GAMBLE AND T. H. GEBALLE, *in* "Treatise on Solid State Chemistry" (N. B. Hannay, Ed.), Vol. 3, Plenum, New York (1976).
7. J. ROUXEL, M. DANOT, AND J. BICHON, *Bull. Soc. Chim. Fr.* **11**, 3930 (1971).
8. M. S. WHITTINGHAM, *Science* **192**, 1126 (1976); *J. Electrochem. Soc.* **123**, 315 (1976).
9. B. G. SILBERNAGEL AND M. S. WHITTINGHAM, *J. Chem. Phys.* **64**, 3670 (1976).
10. B. G. SILBERNAGEL AND M. S. WHITTINGHAM, *Mater. Res. Bull.* **11**, 29 (1978).
11. M. S. WHITTINGHAM, *Progr. Solid State Chem.* **12**, 41 (1978).
12. W. P. F. A. M. OMLOO AND F. JELLINEK, *J. Less Common Metals* **20**, 121 (1970).
13. O. MATSUMOTO, E. YAMADA, Y. KANZAKI, AND M. KONUMA, *J. Phys. Chem. Solids* **39**, 191 (1978).
14. D. A. WINN, J. M. SHEMILT, AND B. C. H. STEELE, *Mater. Tes. Bull.* **11**, 559 (1976).
15. J. A. BENDA, *Phys. Rev. B* **10**, 1409 (1974).
16. A. H. THOMPSON, F. R. GAMBLE, AND R. F. KOEHLER, JR., *Phys. Rev.* **5**, 2811 (1972).
17. F. J. DI SALVO, B. G. BAGLEY, J. M. VOORHOEVE, AND J. V. WASZCZAK, *J. Phys. Chem. Solids* **34**, 1357 (1973).
18. P. J. MESCHTER AND W. L. WORRELL, *Met. Trans. A* **7**, 299 (1976).
19. F. R. GAMBLE, J. H. OSIECKI, AND F. S. DI SALVO, *J. Chem. Phys.* **55**, 3525 (1971).
20. M. S. WHITTINGHAM, *Mater. Res. Bull.* **9**, 1681 (1974).
21. A. LEBLANC-SOREU, M. DANOT, L. TRICHET, AND J. ROUXEL, *Mater. Res. Bull.* **9**, 190 (1974).
22. M. S. WHITTINGHAM AND M. B. DINES, *J. Electrochem. Soc.* **124**, 1387 (1977).
23. E. BAYER AND W. RUDORFF, *Z. Naturforsch. B* **27**, 1336 (1972).
24. A. S. NAGELBERG, Ph.D. dissertation, University of Pennsylvania (1978).
25. D. E. PAUL, D. LIPKIN, AND S. J. WEISSMAN, *J. Amer. Chem. Soc.* **78**, 116 (1956).
26. F. JELLINEK, *J. Less Common Metals* **4**, 9 (1962).
27. A. H. THOMPSON, F. R. GAMBLE, AND C. R. SYMON, *Mater. Res. Bull.* **10**, 915 (1975).
28. S. BASU AND W. L. WORRELL, to be published.
29. R. S. GORDON *et al.*, "N.S.F. Annual Report, Utah–Ford β-Alumina."
30. J. ROUXEL, private communication.
31. S. BASU AND W. L. WORRELL, *in* "Electrode Materials and Processes for Energy Conversion and Storage" (J. D. E. McIntyre, S. Srinivasan, and F. G. Will, Eds.), p. 861, The Electrochemical Society, Princeton, N.J. (1977).
32. H. R. LARSON AND J. F. ELLIOTT, *Trans. AIME* **239**, 1713 (1967).
33. J. L. MARGRAVE, M. S. WHITTINGHAM *et al.*, to be published. Reported by Ref. (*11*).
34. S. S. TODD AND J. P. COUGHLIN, *J. Amer. Chem. Soc.* **74**, 525 (1952).
35. D. W. MURPHY, J. N. CARIDES, F. S. DI SALVO, C. CROS, AND J. V. WASZCZAK, *Mater. Res. Bull.* **12**, 825 (1977).
36. A. S. NAGELBERG AND W. L. WORRELL, to be published.